

Nanostructures | Hot Paper |

Lukas Trombach,^[a] Sergio Rampino,^[b] Lai-Sheng Wang,^[c] and Peter Schwerdtfeger^{*,[d]}

Dedicated to Professor Gernot Frenking on the occasion of his 70th birthday

Abstract: Golden fullerenes have recently been identified by photoelectron spectra by Bulusu et al. [S. Bulusu, X. Li, L.-S. Wang, X. C. Zeng, *PNAS* **2006**, *103*, 8326–8330]. These unique triangulations of a sphere are related to fullerene duals having exactly 12 vertices of degree five, and the icosahedral hollow gold cages previously postulated are related to the Goldberg–Coxeter transforms of C_{20} starting from a triangulated surface (hexagonal lattice, dual of a graphene sheet). This also relates topologically the (chiral) gold nanowires observed to the (chiral) carbon nanotubes. In fact, the Mackay icosahedra well known in gold cluster chemistry are related topologically to the dual halma transforms of the smallest possible fullerene C_{20} . The basic building block here is the (111) fcc sheet of bulk gold which is dual to graphene.

Because of this interesting one-to-one relationship through Euler's polyhedral formula, there are as many golden fullerene isomers as there are fullerene isomers, with the number of isomers N_{iso} increasing polynomially as $O(N_{iso}^2)$. For the recently observed Au_{16}^- , Au_{17}^- , and Au_{18}^- we present simulated photoelectron spectra including all isomers. We also predict the photoelectron spectrum of Au_{32}^- . The stability of the golden fullerenes is discussed in relation with the more compact structures for the neutral and negatively charged Au_{12} to Au_{20} and Au_{32} clusters. As for the compact gold clusters we observe a clear trend in stability of the hollow gold cages towards the (111) fcc sheet. The high stability of the (111) fcc sheet of gold compared to the bulk 3D structure explains the unusual stability of these hollow gold cages.

1. Introduction

Ever since Haruta discovered that gold nanoclusters are catalytically active,^[1–4] we have experienced a new “gold rush” in nanoscience^[5–11] with the discovery of many interesting and often unexpected gold nanostructures.^[12] Gold shows indeed very unusual properties compared to its lighter congeners copper and silver due to pronounced relativistic effects within the Group 11 series of elements.^[13–19] Albeit these effects increase with the expected approximate Z^2 scaling down a group in the periodic table, the late transition metals such as

gold or mercury have rather large relativistic enhancement factors originating from the filling of the underlying valence d-shell.^[18,20] As a result of relativistic effects, smaller gold clusters prefer a planar arrangement,^[21–23] and mixed metal–gold clusters experience strong electron donation toward the gold atoms due to its relativistically increased electronegativity.^[14] This makes mixed gold-cluster systems ideal for electronically fine-tuning chemical and physical properties.^[5] Here we note that the transition of 2D gold triangulated networks to 3D compact gold structures towards the growth into the fcc bulk gold arrangement is the subject of much discussion and debate.^[24–31] In other words, it is currently challenging to understand the growth of metallic clusters toward the bulk by using quantum chemical methods.^[32–34]

Gold clusters can show very unusual and unexpected structures such as the pyramidal Au_{20} cluster^[26,35,36] or the “golden fullerene” I_h-Au_{32} postulated in 2004 by Johansson et al.^[37] This unique I_h-Au_{32} hollow cage can be constructed by replacing each face of the I_h-C_{60} fullerene polyhedron by a gold atom resulting in a triangulated surface of icosahedral symmetry.^[37] More recently, Karttunen et al. predicted a chiral $I-Au_{72}$ cage which is spherically aromatic.^[38] For both copper and silver such a hollow cage becomes rather unstable.^[37,39] A number of such golden fullerenes, that is, $I_h-Au_{32}^-$, $T_d-Au_{16}^-$, $C_{2v}-Au_{17}^-$ and $C_{2v}-Au_{18}^-$, have been identified by photoelectron spectroscopy by Wang and co-workers.^[40,41] Since the publication of the paper by Johansson et al.,^[37] a number of other studies on golden

[a] L. Trombach

Centre for Theoretical Chemistry and Physics, The New Zealand Institute for Advanced Study, Massey University Auckland
Private Bag 102904, 0632 Auckland (New Zealand)

[b] S. Rampino

Istituto di Scienze e Tecnologie Molecolari
Consiglio Nazionale delle Ricerche
c/o Dipartimento di Chimica, Biologia e Biotecnologie
Università degli Studi di Perugia, Via Elce di Sotto 8, 06123 Perugia (Italy)

[c] Prof. L.-S. Wang

Department of Chemistry, Brown University
324 Brook Street, Providence, Rhode Island 02912 (USA)

[d] Prof. P. Schwerdtfeger

Centre for Theoretical Chemistry and Physics, The New Zealand Institute for Advanced Study, Massey University Auckland, Private Bag 102904, 0632 Auckland (New Zealand)
E-mail: p.a.schwerdtfeger@massey.ac.nz

fullerenes have appeared, either with a hollow cage,^[25,34,38,42–49] or with a central metal enclosed^[50–58] extending on the original work of Pyykkö and Runeberg on $W@Au_{12}$.^[59,60] For a recent review see Wang and Wang.^[61]

In this study we explore the relationship between carbon and golden fullerene cages in detail as many interesting topological features known for fullerenes,^[62,63] such as the Goldberg–Coxeter transformation to construct larger fullerene cages,^[64,65] can also be applied to the golden fullerenes. We show that a new class of golden fullerene structures evolves from a one-to-one mapping into the isomer space of fullerene graphs. With this knowledge we reanalyze the experimental photoelectron spectrum of the negatively charged Au_{16}^- cage structure. We also show that stability of such hollow cage structures is not always guaranteed and depends on the sphericity of such systems, but is related to the unusual stability of the (111) fcc sheet of gold. We also explore an interesting topological relationship between Mackay icosahedra and halma transformations recently investigated for fullerenes.^[63]

1.1. Topological aspects

Fullerenes show rich and mathematically interesting topological features,^[62,63] which have been described for example in the works of Fowler and Manolopoulos,^[66] and most recently by our research group in Auckland.^[63] They can be thought of by wrapping a graphene sheet around a sphere (or more generally a genus 0 surface), but introducing 12 pentagons (no more and no less) to fulfil Euler's polyhedral formula:

$$N + F - E = \chi \quad (1)$$

where N is the number of vertices (atoms), F is the number of faces (rings), E is the number of edges (bonds) and χ is called the Euler characteristic with $\chi=2$ for convex polyhedra.^[67] Euler's formula already shows the symmetry between the number of vertices N and the number of faces F , as their role can be interchanged without violating Euler's theorem. Interchanging the roles of vertices and faces in a graphene sheet leads to a (111) sheet (surface) of an (for example) fcc structure adopted in bulk gold (both belonging to the hexagonal 2D lattice group $p3m1$), where the dual vertex is in the center of the hexagon connected by edges to the neighboring dual vertices. Several smaller gold clusters found in the search for global minima are in fact cut-outs from this (111) fcc sheet,^[26] denoted as $p3m1$ -T in the following (Figure 1).

To view it in a different way, the hexagons in the graphene sheets are exactly the Voronoi cells in the $p3m1$ -T sheet. As an interesting side aspect we mention the helical multishell (chiral) gold nanowires found experimentally by Kondo and Takayanagi,^[68] which are duals of multishell (chiral) carbon nanotubes.^[37] These gold nanowires can be constructed exactly in the same way as carbon nanotubes using the chiral vector $C_r(n,m)$ on a hexagonal sheet as described in detail for example by Dresselhaus and co-workers.^[69] As an example we show the D_{6d} fullerene nanotube and its dual structure in Figure 2.

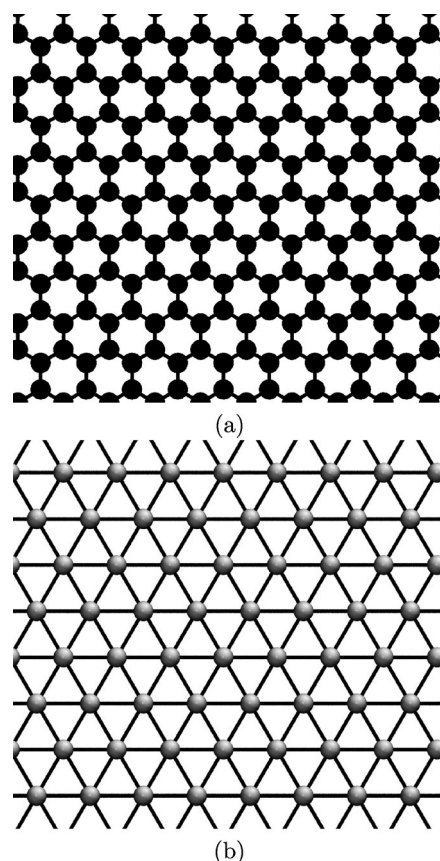


Figure 1. a) $p3m1$ -G graphene, and b) its dual sheet $p3m1$ -T adopted in (111) surface of fcc gold.

The requirement to have 12 pentagons in a fullerene graph with F_h hexagons ($F_h=0$ for C_{20} and $F_h>1$ for all other fullerenes) implies for a fullerene dual to have exactly 12 vertices of degree five and the remaining of degree six. In fact it is well known that C_{22} cannot exist as a fullerene,^[70] which implies that its hypothetical dual Au_{13} does not exist either (the number of vertices N_d in the dual is identical to the number of faces in a fullerene, $N_d = F_f = N_f/2 + 2$,^[63] using subscripts f and d for the fullerene and its dual, respectively). Because there is a one-to-one correspondence between a fullerene and its dual

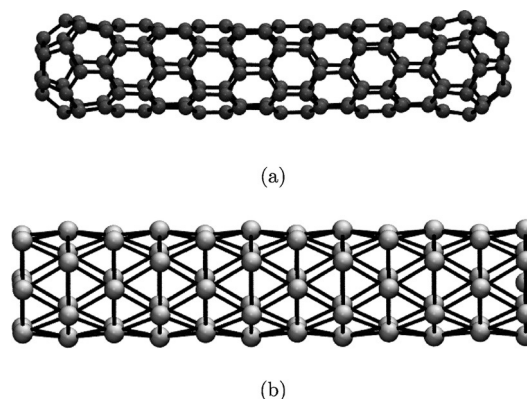


Figure 2. a) D_{6d} - C_{144} zig-zag fullerene nanotube, and b) its dual D_{6d} - Au_{74} .

graph, we have as many isomers (nonisomorphic graphs) for C_{N_f} as we have for $Au_{N_f/2+2}$ and dualization preserves the point group symmetry. Here we mention that according to Thurston, the number of isomers increases polynomially in ninth leading order with the number of vertices, that is, as $O(N_f^9)$.^[71]

Au_{32} was the first of such golden fullerenes postulated by Johansson et al. to be a rather stable hollow cluster, and they were the first ones to mention that these golden dual fullerenes (GDF) are obtained from fullerene graphs.^[37] Au_{32} is shown in Figure 3 together with its dual, C_{60} and the corresponding graph representation (twice the dual transformation leads back to the original polyhedron or graph). Now that we have established an isomorphism between a fullerene graph and its dual, we can easily construct isomers of golden fullerenes by using standard algorithms for the construction of fullerenes, such as the generalized face-spiral algorithm,^[63,66,72,73] embedding the graph on a genus 0 surface and finally transforming the cage to its dual.

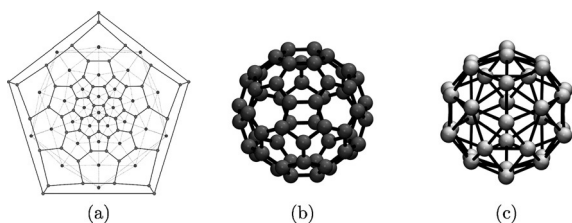


Figure 3. a) Schlegel diagram of C_{60} (red vertices) and its dual (blue vertices and dashed edges), b) the C_{60} structure, and c) its dual Au_{32} structure.

As an example we mention Au_{16} as the dual of C_{28} . Checking the list of possible isomers^[74] we see that there are two possible non-isomorphic structures, D_2-Au_{16} and T_d-Au_{16} . However, only the more symmetric $T_d-Au_{16}^-$ has been considered as a possible candidate in recent photoelectron spectroscopy experiments.^[41] The question naturally arises if the other negatively charged D_2 isomer has a similar photoelectron spectrum and is more stable or not compared to the T_d isomer. In fact, Au_{32} which is the dual of C_{60} has 1812 different isomers with only one fulfilling the isolated pentagon rule (IPR) as proposed by Kroto.^[75] For example, in a recent paper Fa and Dong reported on a hollow gold $D_{6d}-Au_{26}$ cluster.^[25,44] Looking at the list of possible fullerenes we see that there are 199 possible isomers for dual fullerene structures, and in fact there are two possible isomers having D_{6d} symmetry. This just highlights the rich topology of such dual fullerenes.

For the dual structures, we do not know if a similar rule applies, that is an “isolated vertex rule” of degree five (IVR5). In fullerenes the pentagons are responsible for the curvature of the carbon cage and for the overall symmetry and structure, with connected hexagons building planar substructures on the polyhedron. Here we note that the Mackay icosahedron (discussed below) shows exactly that feature.

$p3m1-G$ sheets have been considered by Goldberg and Coxeter for the construction of larger fullerenes.^[64,65,76] The original Goldberg–Coxeter transformation superimposes a hexagonal

mesh on the surface of the C_{20} dodecahedron forming a new polyhedron with leaving the number of pentagons at exactly 12.^[64,65] This transformation can be applied to any fullerene isomer.^[63] The Goldberg–Coxeter transformation $GC_{k,l}$ increases the number of vertices for a fullerene by a factor of $(k^2 + kl + l^2)$, where k and l are integers describing the scale and orientation of the mesh.^[63,76] If $k = l$ or $l = 0$ the point group symmetry is preserved. For example, we have $GC_{1,1}[I_h-C_{20}] = I_h-C_{60}$ (leap-frog transformation)^[66] and $GC_{2,0}[I_h-C_{20}] = I_h-C_{80}$ (halma transformation), or in the dual case applying the same procedure to the $p3m1-T$ sheet for our gold fullerenes $GC_{1,1}[I_h-Au_{12}] = I_h-Au_{32}$ and $GC_{2,0}[I_h-Au_{12}] = I_h-Au_{42}$. Simple algebra shows that $GC_{k,l}[Au_{N_d}]$ has a new vertex count of:

$$N'_d = (k^2 + kl + l^2)(N_d - 2) + 2 \quad (2)$$

Both I_h-Au_{32} and I_h-Au_{42} have been postulated to be stable golden fullerenes before,^[37] and more recently the chiral $I-Au_{72}$ ^[38] which is nothing else but the dual of $GC_{2,1}[I_h-C_{20}] = I-C_{140}$, which is chiral as well as the symmetry being conserved upon dualization.

Now it almost seems trivial to relate Mackay icosahedra^[77] well known for gold clusters^[29,78] to fullerenes. We might call them “multiwalled halma-transformed icosahedral” dual fullerenes in an analogous way to the multiwalled gold nanowires. A Mackay icosahedron is a closed packed multishell structure, each shell being an icosahedron with:

$$N_{\text{shell}} = 10k^2 + 2 \quad (3)$$

number of atoms in each shell with increasing k . This gives the well-known magic cluster numbers of (including the central atom) 13, 55, 147, 309, 561 derived from:

$$N_{\text{total}} = 1 + 2 \sum_{k=1}^{m_{\text{shell}}} (5k^2 + 1) = (10m_{\text{shell}}^3 + 15m_{\text{shell}}^2 + 11m_{\text{shell}} + 3)/3 \quad (4)$$

with $m_{\text{shell}} \geq 1$. One such Mackay icosahedron with $m_{\text{shell}} = 7$ and $N_{\text{total}} = 1415$ is shown in Figure 4. The triangles clearly show the halma pattern of a Goldberg–Coxeter $GC_{k,0}$ transformation. Because each transformation brings a new vertex on the icosahedral edge, we can just deduct the number of shells by counting the number of atoms at one edge of a triangle N_{edger} that is, $m_{\text{shell}} = N_{\text{edger}} - 1$, which gives eight atoms and seven icosahedral shells for the Mackay icosahedron shown in Figure 4. Mackay pointed out that the packing density (or atomic packing factor) for $N \rightarrow \infty$ with $\rho = 0.68818$ is not too different from a closed-packed structure such as fcc with $\rho = \pi/\sqrt{18} = 0.74048$,^[77] one reason why icosahedral cluster growth is often seen. The number of atoms in a shell N_{shell} directly corresponds to the number of faces in a halma transformed C_{20} , that is, for $l = 0$ in the Goldberg–Coxeter transformation and starting with $N_d = 12$ in Equation (2) we have $N'_d = k^2(N_d - 2) + 2 = 10k^2 + 2$ identical with the formula given by Mackay.

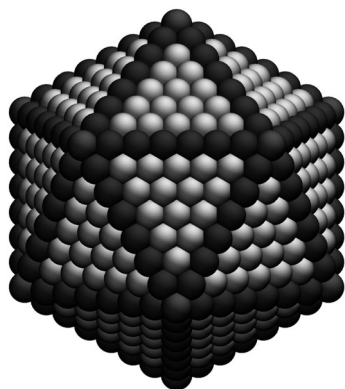


Figure 4. Mackay icosahedron with seven shells and 1415 atoms. The outer icosahedral shell is the dual of the halma transform $GC_{7,0}[I_h-C_{20}] = I_h-C_{980}$.

Finally we note that we can name the different isomers of the golden dual fullerenes exactly in the same way as we do for the fullerenes by using the canonical face spiral pentagon indices (FSPI) and the numbering scheme introduced by Fowler and Manolopoulos,^[66] keeping in mind that the face spiral for fullerenes now becomes a vertex spiral for the dual triangulated surface. We now turn to a detailed analysis of all possible golden dual fullerenes from I_h -Au₁₂, Au₁₄ to Au₂₀ and I_h -Au₃₂ by quantum chemical calculations.

2. Computational Details

Program FULLERENE^[72] was used to construct initial structures of all isomers of the golden dual fullerenes from Au₁₂ to Au₂₀ using a recently developed force-field for fullerenes^[79] (as already mentioned the golden dual fullerene Au₁₃ does not exist). The following isomers need to be considered according to the isomer list for the fullerenes (number in parenthesis gives the number of different isomers of same symmetry):^[72,74] I_h -Au₁₂, D_{6d} -Au₁₄, D_{3h} -Au₁₅, D_2 -Au₁₆, T_d -Au₁₆, D_{5h} -Au₁₇, C_{2v} -Au₁₇(2), D_{3h} -Au₁₈, D_{3d} -Au₁₈, D_3 -Au₁₈, D_2 -Au₁₈, C_3 -Au₁₈(2), C_{3v} -Au₁₉, C_2 -Au₁₉(3), C_5 -Au₁₉(2), D_{6h} -Au₂₀, D_{3h} -Au₂₀, D_{2d} -Au₂₀(2), C_{2v} -Au₂₀, D_2 -Au₂₀(2), C_2 -Au₂₀(3), C_2 -Au₂₀(2), C_1 -Au₂₀(2) and I_h -Au₃₂. The initial force-field optimized structures scaled to an approximate internuclear distance were then refined by using the Perdew–Becke–Ernzerhofer generalized gradient functional^[80,81] corrected for dispersion interactions using Grimme’s method (PBE-D3)^[82,83] together with a Los-Alamos scalar relativistic effective core potential for gold and the accompanying double-zeta basis sets.^[84] Note that the PBE functional was recently considered to perform well for gold clusters.^[85] For several selected clusters we checked that the geometries obtained were accurate by performing calculations using a small core scalar relativistic Stuttgart pseudopotential^[86] together with an augmented valence double-zeta basis set of Peterson and Puzarini.^[87] In comparison, we also calculated the compact global minimum cluster structures which were recently published for the neutral compounds by our group^[26] and for the negatively charged species by Kappes and co-workers.^[88,89]

The simulation of the photoelectron spectra has been carried out by artificial broadening the spectrum of orbital energies with Gaussian functions. The standard deviation σ for these functions was chosen to be 0.035 eV in qualitative agreement with the experimental spectra. The orbital energies were calculated using the PBE density functional with the def2-SVP^[90] double zeta basis implemented in TURBOMOLE 7.0.^[91] The core region was described

using an effective core potential including scalar relativistic effects. The calculated electron affinities were used as the onset value for simulating the photoelectron spectra.

For the calculation of the (111) fcc sheet and the fcc bulk structure of gold we used the program package VASP^[92] utilizing a plane-wave basis set (cutoff energy $E_c = 350$ eV) and the standard projector-augmented wave (PAW) datasets for the elements to model the electron-ion interaction.^[93,94] The electron–electron interaction was modeled within the generalized gradient approximation to the exchange–correlation energy functional as described above and dispersive effects were taken into account by employing Grimme’s D3 dispersion correction with Becke–Johnson damping.^[82,83] Brillouin zone integrations were performed on Γ -centered Monkhorst–Pack grids of k -points with an inverse distance of 0.2 \AA^{-1} . The cohesive energy is defined as the atomization energy per atom keeping in mind that one gold atom is negatively charged for the anionic clusters.

In order to discuss how much the gold cages deviate from sphericity compared to the dual fullerene structure we use the previously introduced definition of a minimum distance sphere (MDS).^[72]

$$\min_{S \in \text{CH}(S)} \frac{1}{N} \sum_i |R_{\text{MDS}} - \|\vec{p}_i - \vec{c}_{\text{MDS}}\|| \quad (5)$$

with the MDS radius defined as:

$$R_{\text{MDS}} = \frac{1}{N} \sum_i \|\vec{p}_i - \vec{c}_{\text{MDS}}\| \quad (6)$$

Here S is the set of n points \vec{p}_i ($i = 1, \dots, N$) in 3-dimensional space, $\text{CH}(S)$ its convex hull, $\|\cdot\|$ the Euclidean norm, and \vec{c}_{MDS} is the barycenter of the MDS with radius R_{MDS} . In other words, we look for a sphere with the vertices lying inside or outside the sphere, but closest to it. We now define a measure for distortion from spherical symmetry through the MDS.^[72]

$$D_{\text{MDS}} = \frac{100}{NR_{\text{min}}} \sum_{i=1}^N |R_{\text{MDS}} - \|\vec{p}_i - \vec{c}_{\text{MDS}}\|| \quad (7)$$

where R_{min} is the smallest bond distance found in the cluster. The pentagon index N_p for a fullerene is defined as:

$$N_p = \frac{1}{2} \sum_{k=1}^5 k p_k \quad \text{with} \quad \sum_{k=0}^5 p_k = 12 \quad (8)$$

where the pentagon indices ($p_l | l = 0, \dots, 5$) define the number of pentagons attached to another pentagon.^[66]

3. Results and Discussion

3.1. Structure and stability

The results for the neutral and negatively charged gold clusters are collected in Table 1 and Table 2, respectively. The dual fullerene structures (DF) are compared to the known global minimum (GM) structures in these tables, and the different isomers are numbered according to their canonical degree 5 vertex spiral identical to the canonical face spiral pentagon indices for fullerenes.^[66] We also include calculations for the most stable neutral and anionic compact Au_{*n*} clusters for comparison which are listed in Table 3. The investigated structures for the

negatively charged gold clusters are depicted in Figure 5 and Figure 6, and the energy differences compared to the global minimum structures are shown in Figure 7.

We can sort out the optimized gold clusters according to whether they can be derived from a dual fullerene structure or not, or more generally from a cubic polyhedral graph. In this case we can simplify Euler's polyhedral formula, which upon dualization (i.e., swapping the role of vertices with faces) gives a triangulation of a sphere obeying the formula:

$$\Gamma = \sum_{n=3} (6-n)N_n = 12 \quad (9)$$

where N_m denotes the number of m -valent vertices. Any deviation from $\Gamma=12$ implies that the polyhedron is not a triangulation of a sphere. For dual fullerenes we only allow for $N_5=12$ and $N_6=0$ or $N_6>1$. Hence we have to look for a complete tri-

angulation and 12 vertices of degree 5 to obtain a dual fullerene structure (also called a geodesic dome).

Table 1 and Table 2 show vertex counts as well as results from Equation (9) for the neutral and anionic clusters, respectively. Considering only the topological parameter Γ it is clear that most of the optimized structures can be derived from a dual planar cubic graph and therefore only consist of triangles. The few notable exceptions are the isomers 12:1 and 20:12 for both the anionic and neutral structure. The ideal icosahedral structure for the Au_{12} cluster is not stable under the present level of theory, and the optimized structure does not correspond to a triangulation of a sphere. However, it has already been shown that this cage can be stabilized by inserting a transition metal (e.g., tungsten) atom into the central position of the icosahedron such that the ten valence electron rule is fulfilled.^[50,59] Addition stabilization of such an endohedral gold cluster can be achieved by attaching ligands to the surface of the cluster.^[96] Structure 20:12 converges towards

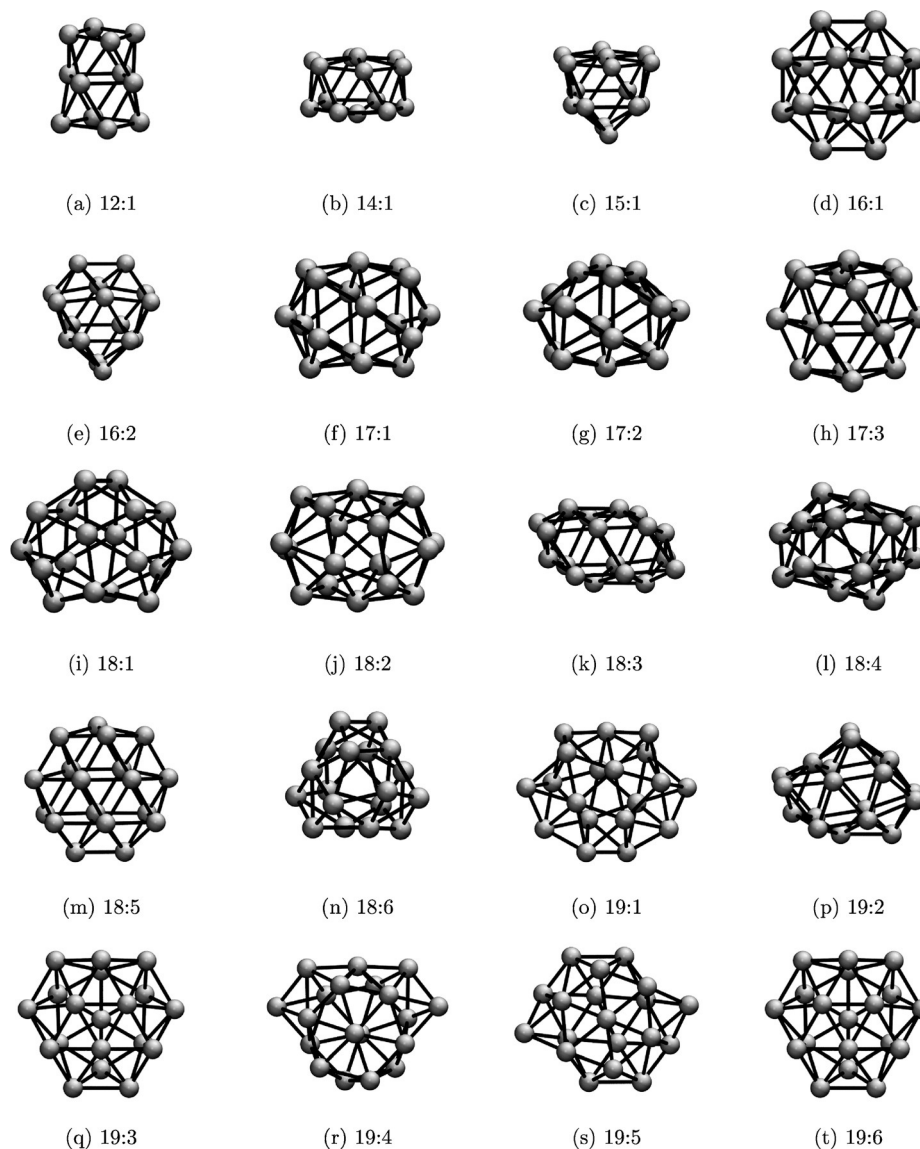


Figure 5. Structures of anionic gold clusters (Au_{12}^- to Au_{19}^-).

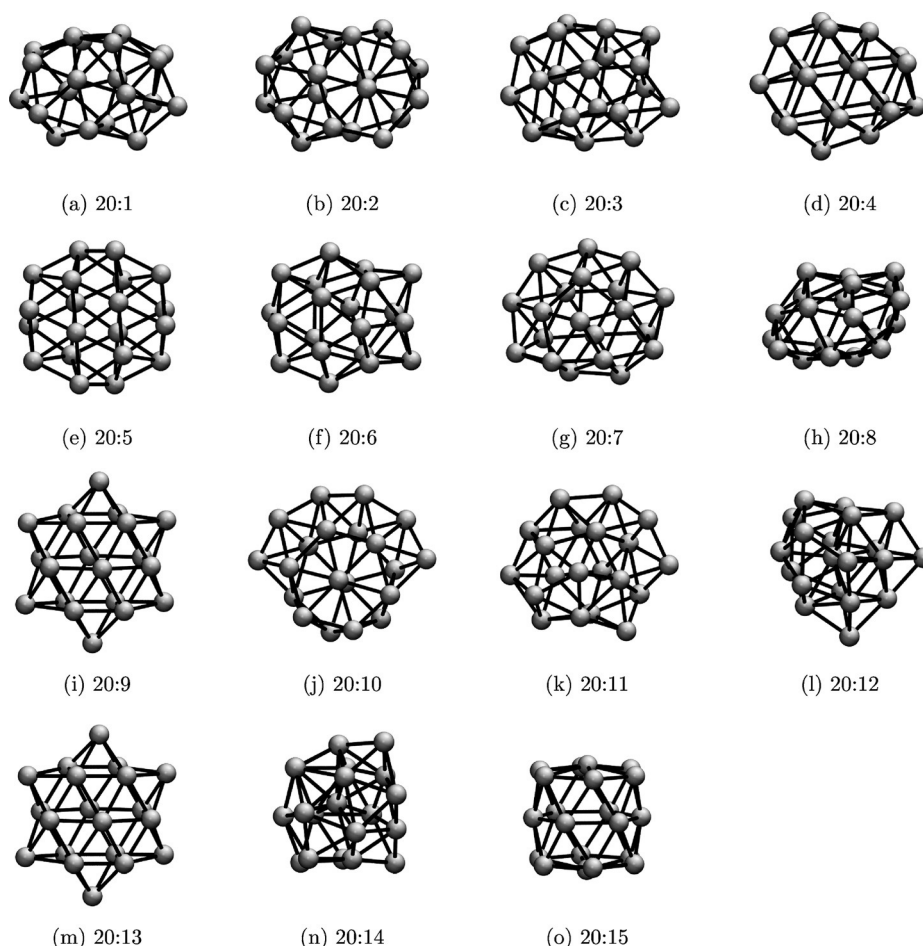


Figure 6. Structures of anionic gold clusters (Au_{20}^-).

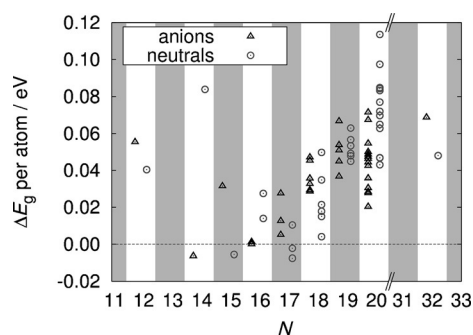


Figure 7. Relative energies for the investigated dual fullerene clusters. Energy differences compared to the most stable compact cluster (per atom) are given in eV.

a more compact cluster with an eightfold coordinated gold atom in the center for both the anionic and the neutral cluster.

Figure 8 gives an overview over all optimized structures. A green field marks a dual fullerene structure with exactly 12 vertices of degree five and the remaining vertices being of degree six. These are also the structures used in Figure 10 and they are more abundant for clusters of size 14 to 19 atoms. Structures with an orange mark do not fulfill the requirement of

being a dual fullerene as they contain vertices of degree 4. However, they are still hollow gold cages and, as mentioned before, show a value of $\Gamma=12$. These structures can be rather similar to the initial dual fullerene structures obtained from a force-field optimization of the corresponding carbon cage, and are usually a result of a flattening towards a more oblate geometry. Most of the clusters shown here preserve their hollow cage structure with only few clusters optimizing into more stable compact structures. These are marked as red in Figure 8.

As illustrated by the distortion parameter $D(F)$ in Tables 2 and 3, carbon fullerenes try to adopt “spherical” shapes if permitted by the distribution of pentagons. This is especially the case for $I_h\text{-C}_{20}$ and $I_h\text{-C}_{60}$ with a distortion parameter of exactly zero (i.e., all atoms lie on a sphere). In contrast, the golden dual fullerene structures have much larger distortion parameters $D(\text{GDF})$ than their carbon equivalent and are therefore less spheroidal. The golden dual fullerenes usually distort into less symmetric structures, for example into oblate structures as mentioned above.

Figure 7 shows the relative energies ΔE_g per atom compared to the most stable compact arrangement for all optimized hollow gold clusters. It is immediately apparent, that the most stable dual fullerene structures can be found in the region of

Table 1. Topological parameters for the neutral gold clusters.^[a]

isomer	Symmetry		Stability		Vertices				Γ	Bond lengths		PI N_p	Distortion	
	ideal	actual	ΔE_n	ΔE_g	N_4	N_5	N_6	N_7		shortest	largest		$D(F)$	$D(GDF)$
12:1	I_h	D_{4h}	-2.058	0.485	8	0	4	0	16	2.798	2.895	30	0	21.1
14:1	D_{6d}	D_{2d}	-2.134	1.173	0	12	2	0	12	2.739	3.048	24	6.1	23.4
15:1	D_{3h}	C_{2v}	-2.192	-0.083	0	12	3	0	12	2.786	2.901	21	5.1	29.2
16:1	D_2	D_2	-2.247	0.223	0	12	4	0	12	2.770	2.917	20	7.9	24.3
16:2	T_d	D_{2d}	-2.233	0.440	0	12	4	0	12	2.716	2.996	18	1.3	28.5
17:1	D_{5h}	C_s	-2.259	0.177	2	8	3	3	12	2.747	3.026	20	11.5	17.3
17:2	C_{2v}	C_{2v}	-2.272	-0.038	0	12	5	0	12	2.769	2.931	18	7.6	19.1
17:3	C_{2v}	C_{2v}	-2.277	-0.128	0	12	5	0	12	2.762	3.139	17	5.5	20.8
18:1	C_2	C_2	-2.307	0.321	0	12	6	0	12	2.736	2.934	17	9.2	16.9
18:2	D_2	D_2	-2.290	0.627	0	12	6	0	12	2.733	2.935	18	11.6	17.2
18:3	D_{3d}	D_{3d}	-2.275	0.896	0	12	6	0	12	2.714	2.894	18	12.1	18.2
18:4	C_2	C_2	-2.321	0.073	0	12	6	0	12	2.749	2.931	16	7.2	18.7
18:5	D_{3h}	D_{3h}	-2.303	0.386	0	12	6	0	12	2.763	3.159	8	15.1	27.3
18:6	D_3	D_3	-2.310	0.270	0	12	6	0	12	2.742	2.945	15	5.8	15.2
19:1	C_2	C_2	-2.298	1.196	0	12	7	0	12	2.745	3.006	17	14.9	26.0
19:2	C_s	C_s	-2.307	1.014	0	12	7	0	12	2.747	2.972	15	7.5	20.0
19:3	C_s	C_s	-2.304	1.077	0	12	7	0	12	2.737	2.957	15	11.9	28.3
19:4	C_2	C_2	-2.311	0.935	0	12	7	0	12	2.745	2.905	15	7.0	17.7
19:5	C_2	C_2	-2.313	0.911	0	12	7	0	12	2.734	2.947	14	6.6	18.7
19:6	C_{3v}	C_{3v}	-2.316	0.854	0	12	7	0	12	2.765	2.890	15	12.7	30.6
20:1	C_2	C_1	-2.324	1.684	2	8	10	0	12	2.711	2.984	16	15.3	36.7
20:2	D_2	D_2	-2.295	2.271	0	12	8	0	12	2.699	3.023	18	20.4	22.0
20:3	C_1	C_1	-2.339	1.395	2	8	10	0	12	2.724	2.954	15	13.1	129.1
20:4	C_s	C_s	-2.324	1.695	0	12	8	0	12	2.709	3.023	16	13.7	25.5
20:5	D_2	D_2	-2.332	1.541	0	12	8	0	12	2.749	3.080	16	18.5	17.3
20:6	D_{2d}	C_{2v}	-2.337	1.440	2	8	10	0	12	2.752	2.977	14	9.8	26.6
20:7	C_1	C_1	-2.325	1.663	2	9	8	1	12	2.712	3.019	14	10.9	25.8
20:8	C_s	C_s	-2.346	1.256	2	8	10	0	12	2.748	3.057	14	8.4	40.7
20:9	C_{2v}	D_{6h}	-2.362	0.938	6	0	14	0	12	2.744	2.971	13	3.8	23.2
20:10	C_2	C_2	-2.344	1.299	2	8	10	0	12	2.726	3.004	14	12.6	23.9
20:11	C_2	C_s	-2.346	1.256	2	8	10	0	12	2.747	3.056	13	8.1	35.8
20:12	C_2	C_1	-2.366	0.861	3	5	4	7	4	2.719	3.048	13	5.4	21.1
20:13	D_{3h}	D_{6h}	-2.362	0.938	6	0	14	0	12	2.744	2.970	15	6.5	27.9
20:14	D_{2d}	D_{2d}	-2.311	1.948	0	12	8	0	12	2.779	2.929	12	3.7	22.0
20:15	D_{6h}	D_{6h}	-2.362	0.936	6	0	14	0	12	2.744	2.972	12	4.5	25.6
32:1082	I_h	I_h	-2.494	1.537	0	12	20	0	12	2.793	2.835	0	0	7.5
(111)	2D	sheet	-2.994	-	0	0	∞	0	-	2.722	2.722	0	0	0
fcc	3D	bulk	-3.677	-	-	-	-	-	-	2.897	2.897	-	-	-

[a] Number of gold atoms and isomer numbers of the corresponding fullerene in canonical order of the pentagon spiral indices,^[66] ideal and actual point group symmetry, energy differences ΔE_g to the most stable neutral cluster of same size and binding energy per atom $\Delta E_n = [E(Au_n) - nE(Au)]/n$ [eV], shortest and largest bond distance [Å], pentagon index (PI) N_p , and distortion parameter D (in %) for the initial force-field optimized fullerene structure (F) and the dual gold cluster (GDF).

14 to 18 atoms. Some clusters in this region even exceed the stability of formerly proposed global minimum structures. For example, for Au_{16}^- the global minimum has been proposed before to be the tetrahedral hollow cluster^[88,89] which is the dual of the tetrahedral C_{28} isomer as observed experimentally in photoelectron spectra.^[41] We should mention, that Chen et al. have found the tetrahedral structure to lie 0.22 eV above a sheet-like structure.^[46] However, our results contradict these findings as the planar structure is predicted to be 0.939 eV higher in energy. Here we point out that according to our calculations the D_2 symmetric isomer 16:1 lies only 0.02 eV above the tetrahedral structure. Therefore, it should also be possible to observe this isomer by experimental methods.

Possible Au_{32} structures have been investigated intensively by Jalbout et al.^[95] We compare our results to the most stable

isomers found in their work (Table 3). For both neutral and anionic clusters, isomer 10 in their work (see ref. [95] for details) turns out to be the most stable compact geometry and the icosahedral hollow structure 32:1082 is less stable in both cases, that is, for the neutral and anionic cluster. We also include the C_{3v} compact structure in Table 3 not investigated before, which is derived from the ideal Au_{35} tetrahedron by removing three of the corner atoms in the tetrahedron and can be seen as a cut-out of the fcc bulk structure. This cluster is also very stable compared to the other structures proposed by Jalbout et al. We also mention that the Au_{32} hollow cage distorts from an ideal icosahedral symmetry into a D_{2h} arrangement, which is reflected in the distortion parameter $D(Au_{32}) = 10.4$, which however is rather small. Au_{32} can therefore be seen as pseudospherical.

Table 2. Topological parameters for the anionic gold clusters.

isomer	Symmetry		Stability		N_4	Vertices				Γ	Bond lengths		Distortion $D(\text{GDF})$
	ideal	actual	ΔE_n	ΔE_g		N_5	N_6	N_7	shortest		largest		
12:1	I_h	D_{2d}	-2.137	0.665	8	0	4	0	16	2.780	2.869	23.0	
14:1	D_{6d}	D_{2d}	-2.242	-0.089	0	12	2	0	12	2.758	2.989	20.3	
15:1	D_{3h}	C_{2v}	-2.281	0.473	0	12	3	0	12	2.741	3.029	21.2	
16:1	D_2	D_2	-2.328	0.020	0	12	4	0	12	2.764	2.905	17.7	
16:2	T_d	D_{2d}	-2.330	0.000	0	12	4	0	12	2.738	2.907	16.2	
17:1	D_{5h}	D_{5h}	-2.353	0.469	0	12	5	0	12	2.757	3.017	13.2	
17:2	C_{2v}	C_{2v}	-2.368	0.215	0	12	5	0	12	2.742	2.994	14.4	
17:3	C_{2v}	C_{2v}	-2.376	0.087	0	12	5	0	12	2.731	3.019	14.2	
18:1	C_2	C_2	-2.360	0.589	0	12	6	0	12	2.734	2.968	16.8	
18:2	D_2	C_2	-2.346	0.848	0	12	6	0	12	2.733	3.059	16.8	
18:3	D_{3d}	C_2	-2.348	0.817	4	4	10	0	12	2.701	3.038	24.3	
18:4	C_2	C_1	-2.364	0.529	0	12	6	0	12	2.740	3.048	19.0	
18:5	D_{3h}	D_{3h}	-2.364	0.516	0	12	6	0	12	2.710	3.023	27.5	
18:6	D_3	D_3	-2.357	0.642	0	12	6	0	12	2.734	2.912	14.7	
19:1	C_2	C_2	-2.384	0.967	4	4	11	0	12	2.732	2.985	28.5	
19:2	C_2	C_2	-2.368	1.268	2	9	7	1	12	2.727	2.989	16.9	
19:3	C_5	C_{3v}	-2.381	1.022	0	12	7	0	12	2.755	3.046	32.6	
19:4	C_2	C_2	-2.390	0.853	2	8	9	0	12	2.744	3.003	22.1	
19:5	C_2	C_2	-2.398	0.698	2	8	9	0	12	2.743	2.963	31.3	
19:6	C_{3v}	C_{3v}	-2.381	1.023	0	12	7	0	12	2.756	3.044	32.4	
20:1	C_2	C_1	-2.386	0.927	2	8	10	0	12	2.748	3.032	25.0	
20:2	D_2	D_2	-2.365	1.348	0	12	8	0	12	2.731	2.971	43.8	
20:3	C_1	C_1	-2.396	0.716	2	8	10	0	12	2.745	2.926	23.4	
20:4	C_5	C_5	-2.385	0.950	0	12	8	0	12	2.740	2.939	24.4	
20:5	D_2	D_2	-2.390	0.850	0	12	8	0	12	2.775	2.907	37.4	
20:6	D_{2d}	C_2	-2.382	1.001	2	8	10	0	12	2.770	2.948	20.5	
20:7	C_1	C_1	-2.384	0.974	0	12	8	0	12	2.739	3.079	25.3	
20:8	C_5	C_5	-2.388	0.888	2	8	10	0	12	2.761	2.977	22.0	
20:9	C_{2v}	D_{6h}	-2.402	0.610	6	0	14	0	12	2.731	2.971	27.1	
20:10	C_2	C_2	-2.404	0.568	2	8	10	0	12	2.743	2.984	37.1	
20:11	C_2	C_1	-2.378	1.093	3	8	7	2	12	2.732	3.018	26.5	
20:12	C_2	C_5	-2.412	0.407	2	8	3	6	6	1.755	2.996	192.0	
20:13	D_{3h}	D_{6h}	-2.402	0.610	6	0	14	0	12	2.731	2.972	27.0	
20:14	D_{2d}	C_1	-2.405	0.544	2	8	1	8	12	2.710	3.010	199.2	
20:15	D_{6h}	D_{6h}	-2.361	1.430	0	12	8	0	12	2.792	2.933	15.2	
32:1082	I_h	D_{2h}	-2.524	2.201	0	12	20	0	12	2.766	3.004	10.4	

[a] Number of gold atoms and isomer numbers of the fullerene in canonical order of the pentagon spiral indices,^[66] ideal and actual point group symmetry, energy differences ΔE_g to the most stable anionic cluster of same size and binding energy per atom $\Delta E_n = [E(\text{Au}_n) - (n-1)E(\text{Au}) - E(\text{Au}^-)]/n$ [eV], shortest and largest bond distance [\AA], and distortion parameter D [%] for the dual gold cluster (GDF).

Table 3. Binding energy per atom [eV] for investigated neutral and anionic compact cluster compounds.^[a]

N	Symmetry	$\Delta E_n(\text{neutral})$	N	Symmetry	$\Delta E_n(\text{neutral})$	N	Symmetry	$\Delta E_n(\text{anion})$
2	$D_{\infty h}$	-1.105	13	C_{2v}	-2.087	12	D_{3h}	-2.192
3	C_{2v}	-1.152	14	C_{2v}	-2.218	14	D_{2h}	-2.236
4	D_{2h}	-1.486	15	C_5	-2.186	15	C_1	-2.313
5	C_{2v}	-1.631	16	C_5	-2.261	16	D_{2d}	-2.330
6	D_{3h}	-1.875	17	C_5	-2.270	17	C_{2v}	-2.381
7	C_5	-1.833	18	C_5	-2.325	18	C_{2v}	-2.393
8	D_{4h}	-1.959	19	C_{3v}	-2.361	19	C_{3v}	-2.435
9	C_{2v}	-1.944	20	T_d	-2.409	20	T_d	-2.432
10	D_{2h}	-2.028	32	C_{3v}	-2.491	32	C_{3v}	-2.548
11	D_{3h}	-2.063	32	isomer1	-2.536	32	isomer1	-2.590
12	D_{3h}	-2.098	32	isomer10	-2.542	32	isomer10	-2.593

[a] For the definition of the binding energy see Table 1 and Table 2, and for the definition of the isomer 1 and 10 for Au_{32} see reference [95].

3.2. Convergence towards the infinite structure

The neutral gold clusters and their property convergence towards the bulk has already been discussed in one of our previous papers.^[26] Increasing the size of non-hollow compact clusters lowers the cohesive energy until the clusters are large enough to be a valid representation of the bulk gold structure. This can be seen in Figure 9, where a clear linear correlation between cluster size and the cohesive energy is depicted.

Hollow gold clusters can be created by wrapping a cutout from a (111) gold 2D sheet around a sphere introducing 12 vertices of degree 5 to satisfy Euler's theorem. Therefore, an infinitely large 2D gold sheet represents a golden dual fullerene cage with an infinite sphere radius. As the cohesive energy of the compact structures converges towards the bulk cohesive energy, the cohesive energy of the 2D gold sheet

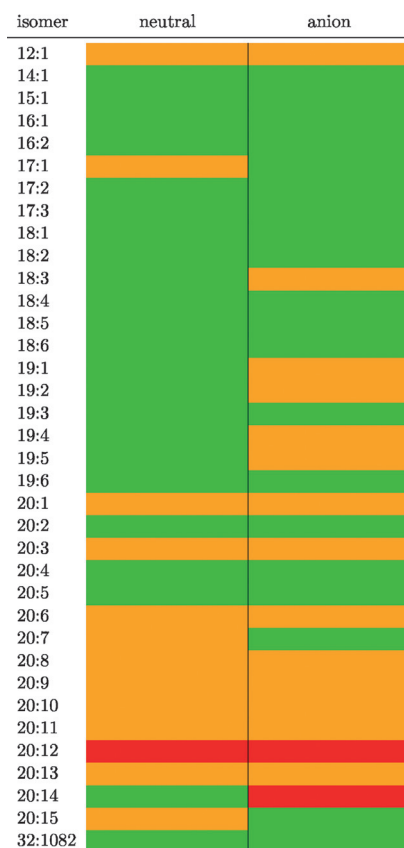


Figure 8. Overview of PBE-D3 optimization results for the dual fullerene structures. Green: dual fullerene structure, orange: hollow structure, red: non-hollow structure.

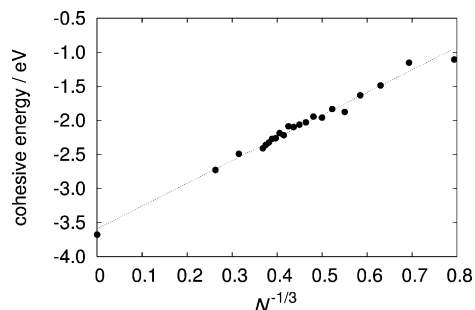


Figure 9. Cohesive energies for the compact gold clusters with cluster size N and convergence toward the bulk fcc structure.

should represent the infinite limit for the dual golden fullerene structures. This is indeed the case and is depicted in Figure 10 using a N^{-1} scaling law analogue to the one used for fullerenes (for details see ref. [79]).

An interesting result here is the difference between the cohesive energy of the bulk fcc structure compared to the (111) 2D sheet. Creating the bulk structure from stacking (111) sheets only accounts for approximately 0.68 eV of the total cohesive energy of the bulk which is 3.81 eV.^[97] This implies that most of the cohesive energy of bulk gold originates from the (111) sheet, which is therefore exceptionally stable and can be seen as a reason for the preferred planar arrangement of many

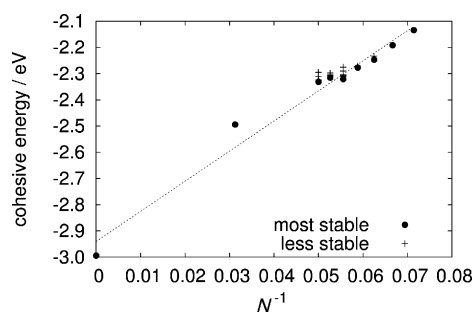


Figure 10. Cohesive energies for the hollow gold clusters with cluster size N and convergence toward the (111) gold sheet.

small gold clusters. As pointed out by Takeuchi et al., relativistic effects increase the cohesive energy of bulk gold by 1.5 eV.^[97] A similar large relativistic effect is expected for the (111) sheet of gold.

3.3. Simulation of photoelectron spectra

Photoelectron spectra of several golden cages dual fullerenes have been determined experimentally and simulated by theoretical methods by Bulusu et al.^[41] Before we discuss our results we need to consider spin-orbit effects as substantial 5d-mixing into the 6s orbitals of gold occurs in such clusters. Figure 11 shows a comparison of simulated photoelectron spectra of the three golden dual fullerene isomers of Au_{17}^- . The results clearly show that spin-orbit effects can be neglected in this energy range.

Bulusu et al. considered only the $\text{Au}_{16}^- T_d$ structure. From our data there is reason to believe that the other possible isomer 16:1 is also present in the measured spectrum. Figure 12 shows our simulation results for the isomers 16:1 and 16:2 and a simulation for a mixture of both compounds with a ratio of 1:1 as the energy of both isomers are comparable. Looking at the experimental data a shoulder can be identified in the first peak. We can reproduce this feature by shifting the spectra for 16:1 and 16:2 according to the corresponding vertical ionization potential, superimposing both spectra and shift the result by 0.18 eV to better fit the experimental data as pictured in Figure 12. This indicates that the second hollow cage isomer has also been produced. Further evidence for this could be the experimental peak at 5.51 eV. The simulated spectrum for the tetrahedral cluster shows a dip at this energy, while the D_2 structure has a clear intensity maximum.

Figure 12 shows the simulated spectra for the three possible dual fullerene isomers for Au_{17}^- . The spectra have been shifted according to the vertical ionization potential of the negatively charged clusters. The most stable structures are 17:2 (red) and 17:3 (green) of which 17:2 fits reasonably well for the first four peaks. The peak at 4.73 eV could be accounted to the 17:3 isomer which is identical to Bulusu and co-workers' C_{2v} symmetric structure.

From the relative energies in Figure 7 it is clear that anionic dual fullerene structures start to become rather unstable for $N=18$. Therefore, compact clusters might dominate the experi-

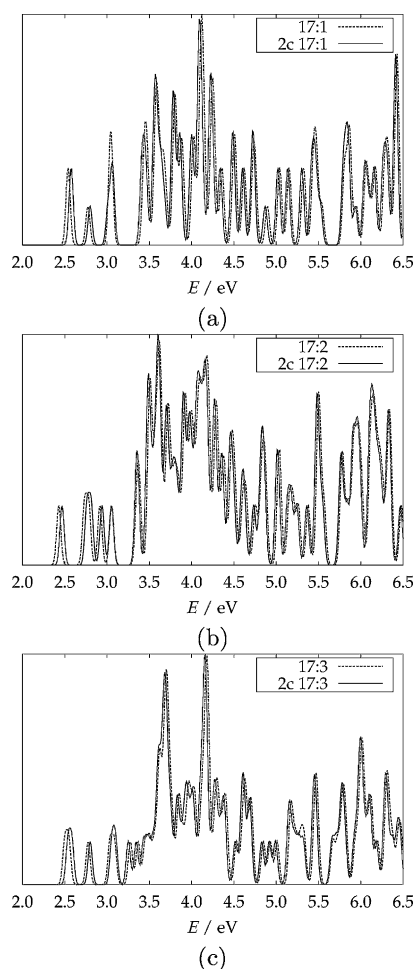


Figure 11. Comparison of simulated photoelectron spectra of the three dual fullerene isomers of Au_{17}^- with (2c) and without spin-orbit coupling.

mental spectrum. Figure 12 shows our calculated spectra in comparison with the experimental data. The calculated spectra have been first shifted to the corresponding vertical ionization potential and subsequently shifted by 0.25 eV to better fit the experimental data. The most stable dual fullerene clusters are 18:1, 18:4 and 18:5; 18:1 and 18:5 could be responsible for the second peak in the experimental data at 3.63 eV, while 18:4 agrees with the first peak. The signal at 3.97 eV could be an indication that isomer 18:3 was produced as it is the only structure that shows a peak in that area, although it is the least stable of the hollow structures.

Finally, for future experiments we include our simulated photoelectron spectrum for Au_{32}^- which is shown in Figure 13.

4. Summary

We found an interesting topological relationship between fullerenes and the cage-like gold clusters resulting in a triangulation of a sphere with vertices of degrees 5 and 6 fulfilling Euler's polyhedral formula. Because of this isomorphism between the two structures by dualization, there are as many golden fullerene isomers as there are different fullerene struc-

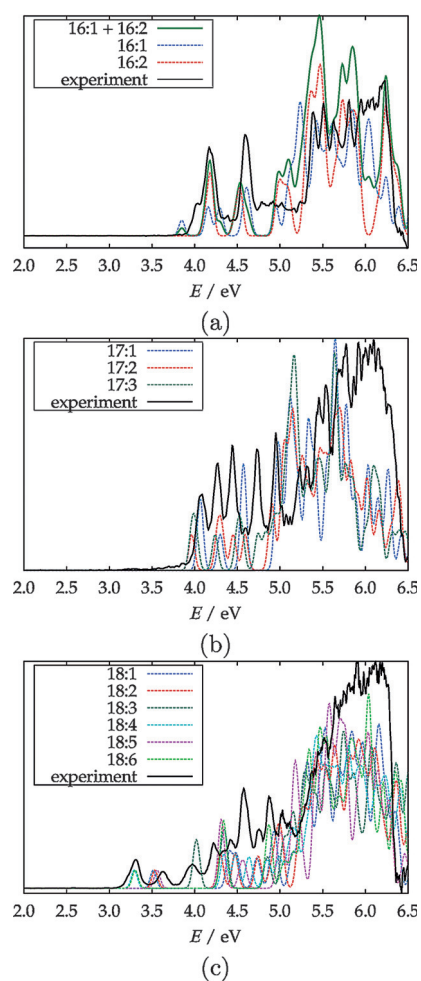


Figure 12. Simulated photoelectron spectra for the negatively charged hollow gold clusters (shifted to the experimental threshold energy). a) The two possible dual fullerene isomers of Au_{16}^- . The green curve shows a combination of the D_2 and T_d spectra with a ratio of 1:1. b) The three possible dual fullerene isomers of Au_{17}^- . c) The six possible dual fullerene isomers of Au_{18}^- (shifted to the experimental threshold energy).

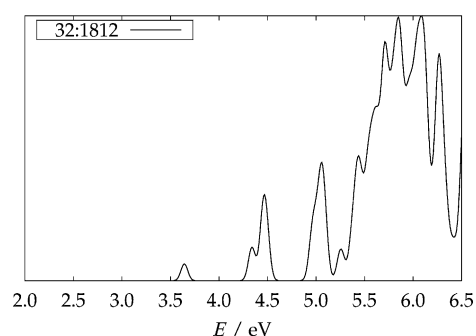


Figure 13. Simulated photoelectron spectra for 32:1812 isomer of Au_{32}^- .

tures. In the same way we relate gold nanotubes to carbon nanotubes and halma transforms of C_{20} to the shells of a Mackay icosahedron. We investigated the stability of these golden fullerenes. While they perhaps may not compete in energy with the more compact gold clusters at larger cluster size,^[98] the smaller cage structures are stable as observed by

photoelectron spectroscopy. Our simulated photoelectron spectra suggest that more than one golden fullerene isomer was observed. A natural step in the next direction would be to stabilize such hollow gold clusters by either endohedral enclosure of gold or other metal atoms or by attaching appropriate ligands to the outside of the cage.

Acknowledgements

P.S. thanks Prof. Nobuhiko Sarukura (Osaka) and the Alexander von Humboldt Foundation (Bonn) for financial support. We also thank Profs. Pekka Pyykkö and Dage Sundholm (Helsinki), Leonardo Belpassi and Lorian Storch (Perugia) for interesting discussions, and Dr. X. G. Gong for the Au₅₈ cluster data.

Keywords: Goldberg–Coxeter transforms · golden dual fullerenes · nanostructures · photoelectron spectroscopy · topology

- [1] M. Haruta, T. Kobayashi, H. Sano, N. Yamada, *Chem. Lett.* **1987**, 16, 405.
- [2] M. Haruta, *Chem. Rec.* **2003**, 3, 75.
- [3] T. Ishida, M. Haruta, *Angew. Chem. Int. Ed.* **2007**, 46, 7154; *Angew. Chem.* **2007**, 119, 7288.
- [4] M. Haruta, *ChemPhysChem* **2007**, 8, 1911.
- [5] P. Schwerdtfeger, *Angew. Chem. Int. Ed.* **2003**, 42, 1892; *Angew. Chem.* **2003**, 115, 1936.
- [6] H. Häkkinen, *Chem. Soc. Rev.* **2008**, 37, 1847–1859.
- [7] P. Maity, S. Xie, M. Yamauchi, T. Tsukuda, *Nanoscale* **2012**, 4, 4027–4037.
- [8] Y. Zhang, X. Cui, F. Shi, Y. Deng, *Chem. Rev.* **2012**, 112, 2467–2505.
- [9] J. Gong, *Chem. Rev.* **2012**, 112, 2987–3054.
- [10] M.-S. Miao, J. A. Kurzman, N. Mammen, S. Narasimhan, R. Seshadri, *Inorg. Chem.* **2012**, 51, 7569–7578.
- [11] K. Park, L. F. Drummy, R. C. Wadams, H. Koerner, D. Nepal, L. Fabris, R. A. Vaia, *Chem. Mater.* **2013**, 25, 555–563.
- [12] Y. Chen, C. Zeng, C. Liu, K. Kirschbaum, C. Gayathri, R. R. Gil, N. L. Rosi, R. Jin, *J. Am. Chem. Soc.* **2015**, 137, 10076–10079.
- [13] P. Pyykkö, *Chem. Rev.* **1988**, 88, 563–594.
- [14] P. Schwerdtfeger, *Heteroat. Chem.* **2002**, 13, 578–584.
- [15] P. Pyykkö, *Angew. Chem. Int. Ed.* **2004**, 43, 4412–4456; *Angew. Chem.* **2004**, 116, 4512–4557.
- [16] P. Pyykkö, *Nat. Nanotechnol.* **2007**, 2, 273–274.
- [17] W. Huang, M. Ji, C.-D. Dong, X. Gu, L.-M. Wang, X. G. Gong, L.-S. Wang, *ACS Nano* **2008**, 2, 897–904.
- [18] P. Schwerdtfeger, M. Lein, *Theoretical Chemistry of Gold From Atoms to Molecules, Clusters, Surfaces and the Solid State*, Wiley-VCH, Weinheim, **2009**, pp. 183–247.
- [19] P. Pyykkö, *Annu. Rev. Phys. Chem.* **2012**, 63, 45–64.
- [20] J. Autschbach, S. Siekierski, M. Seth, P. Schwerdtfeger, W. H. E. Schwarz, *J. Comput. Chem.* **2002**, 23, 804–813.
- [21] G. Bravo-Pérez, I. L. Garzón, O. Novaro, *J. Mol. Struct. THEOCHEM* **1999**, 493, 225.
- [22] H. Häkkinen, U. Landman, *Phys. Rev. B* **2000**, 62, R2287.
- [23] H. Häkkinen, M. Moseler, U. Landman, *Phys. Rev. Lett.* **2002**, 89, 033401.
- [24] M. P. Johansson, A. Lechtken, D. Schooss, M. M. Kappes, F. Furche, *Phys. Rev. A* **2008**, 77, 053202.
- [25] W. Fa, C. Luo, J. Dong, *Phys. Rev. B* **2005**, 72, 205428.
- [26] B. Assadollahzadeh, P. Schwerdtfeger, *J. Chem. Phys.* **2009**, 131, 064306.
- [27] L.-M. Wang, R. Pal, W. Huang, X. C. Zeng, L.-S. Wang, *J. Chem. Phys.* **2010**, 132, 114306.
- [28] B. Wang, M. Liu, Y. Wang, X. Chen, *J. Phys. Chem. C* **2011**, 115, 11374–11381.
- [29] F. Furche, R. Ahlrichs, P. Weis, C. Jacob, S. Gilb, T. Bierweiler, M. M. Kappes, *J. Chem. Phys.* **2002**, 117, 6982–6990.
- [30] A. S. Barnard, *Acc. Chem. Res.* **2012**, 45, 1688–1697.
- [31] D. A. Götz, R. Schäfer, P. Schwerdtfeger, *J. Comput. Chem.* **2013**, 34, 1975–1981.
- [32] H.-Y. Zhao, H. Ning, J. Wang, X.-J. Su, X.-G. Guo, Y. Liu, *Phys. Lett. A* **2010**, 374, 1033–1038.
- [33] A. S. Barnard, *Rep. Prog. Phys.* **2010**, 73, 086502.
- [34] D. Tian, J. Li, Y. Zhao, J. Zhao, X. Guo, *Comput. Mater. Sci.* **2011**, 50, 2359–2362.
- [35] J. Li, X. Li, H.-J. Zhai, L.-S. Wang, *Science* **2003**, 299, 864–867.
- [36] P. Gruene, D. M. Rayner, B. Redlich, A. F. G. van der Meer, J. T. Lyon, G. Meijer, A. Fielicke, *Science* **2008**, 321, 674–676.
- [37] M. P. Johansson, D. Sundholm, J. Vaara, *Angew. Chem. Int. Ed.* **2004**, 43, 2678–2681; *Angew. Chem.* **2004**, 116, 2732–2735.
- [38] A. J. Karttunen, M. Linnolahti, T. A. Pakkanen, P. Pyykkö, *Chem. Commun.* **2008**, 465–467.
- [39] E. M. Fernández, M. B. Torres, L. C. Balbás, in *Prog. Theoret. Chem. Phys., Vol. 15 of Recent Advances in the Theory of Chemical and Physical Systems* (Eds.: J.-P. Julien, J. Maruani, D. Mayou, S. Wilson, G. Delgado-Barrio), Springer, Amsterdam, **2006**, pp. 407–432.
- [40] M. Ji, X. Gu, X. Li, X. Gong, J. Li, L.-S. Wang, *Angew. Chem. Int. Ed.* **2005**, 44, 7119–7123; *Angew. Chem.* **2005**, 117, 7281–7285.
- [41] S. Bulusu, X. Li, L.-S. Wang, X. C. Zeng, *Proc. Natl. Acad. Sci. USA* **2006**, 103, 8326–8330.
- [42] X. Gu, M. Ji, S. H. Wei, X. G. Gong, *Phys. Rev. B* **2004**, 70, 205401.
- [43] E. M. Fernández, J. M. Soler, L. C. Balbás, *Phys. Rev. B* **2006**, 73, 235433.
- [44] W. Fa, J. Dong, *J. Chem. Phys.* **2006**, 124, 114310.
- [45] W. Fa, J. Zhou, C. Luo, J. Dong, *Phys. Rev. B* **2006**, 73, 085405.
- [46] G. Chen, Q. Wang, Q. Sun, Y. Kawazoe, P. Jena, *J. Chem. Phys.* **2010**, 132, 194306.
- [47] H. S. De, S. Krishnamurty, S. Pal, *Catal. Today* **2012**, 198, 106–109; special Issue dedicated to Paul Ratnasamy on the occasion of his 70th birthday.
- [48] H. Ning, J. Wang, Q.-M. Ma, H.-Y. Han, Y. Liu, *J. Phys. Chem. Solids* **2014**, 75, 696–699.
- [49] K. Joshi, S. Krishnamurty, *Mol. Phys.* **2015**, 113, 2980–2991.
- [50] J. Autschbach, B. A. Hess, M. P. Johansson, J. Neugebauer, M. Patzschke, P. Pyykkö, M. Reiher, D. Sundholm, *Phys. Chem. Chem. Phys.* **2004**, 6, 11–22.
- [51] H.-J. Zhai, J. Li, L.-S. Wang, *J. Chem. Phys.* **2004**, 121, 8369–8374.
- [52] Y. Gao, S. Bulusu, X. C. Zeng, *J. Am. Chem. Soc.* **2005**, 127, 15680–15681.
- [53] L.-M. Wang, S. Bulusu, W. Huang, R. Pal, L.-S. Wang, X. C. Zeng, *J. Am. Chem. Soc.* **2007**, 129, 15136–15137.
- [54] L.-M. Wang, S. Bulusu, H.-J. Zhai, X.-C. Zeng, L.-S. Wang, *Angew. Chem. Int. Ed.* **2007**, 46, 2915–2918; *Angew. Chem.* **2007**, 119, 2973–2976.
- [55] W. Fa, J. Dong, *J. Chem. Phys.* **2008**, 128, 144307.
- [56] A. Munoz-Castro, *J. Phys. Chem. Lett.* **2013**, 4, 3363–3366.
- [57] D. Manna, T. Jayasekharan, T. K. Ghanty, *J. Phys. Chem. C* **2013**, 117, 18777–18788.
- [58] C. Tang, W. Zhu, A. Zhang, K. Zhang, M. Liu, *Comput. Theor. Chem.* **2013**, 1018, 1–5.
- [59] P. Pyykkö, N. Runeberg, *Angew. Chem. Int. Ed.* **2002**, 41, 2174–2176; *Angew. Chem.* **2002**, 114, 2278–2280.
- [60] X. Li, B. Kiran, J. Li, H.-J. Zhai, L.-S. Wang, *Angew. Chem. Int. Ed.* **2002**, 41, 4786–4789; *Angew. Chem.* **2002**, 114, 4980–4983.
- [61] L.-M. Wang, L.-S. Wang, *Nanoscale* **2012**, 4, 4038–4053.
- [62] F. Cataldo, A. Graovac, O. Ori, *The Mathematics and Topology of Fullerenes*, Springer, Berlin, **2011**.
- [63] P. Schwerdtfeger, L. N. Wirz, J. Avery, *WIREs Comput. Mol. Sci.* **2015**, 5, 96–145.
- [64] M. Goldberg, *Tohoku Math. J.* **1937**, 43, 104–108.
- [65] H. S. M. Coxeter, in *A Spectrum of Mathematics: Essays Presented to H. G. Forder* (Ed.: J. C. Butcher), Oxford University Press, Oxford, **1971**, pp. 98–107.
- [66] P. W. Fowler, D. E. Manolopoulos, in *An Atlas of Fullerenes*, 2nd ed., Dover, Mineola, **2006**.
- [67] D. Kotschick, *Am. Sci.* **2006**, 94, 350–357.
- [68] Y. Kondo, K. Takayanagi, *Science* **2000**, 289, 606–608.
- [69] M. Fujita, R. Saito, G. Dresselhaus, M. S. Dresselhaus, *Phys. Rev. B* **1992**, 45, 13834–13836.
- [70] G. Grünbaum, T. S. Motzkin, *Can. J. Math.* **1963**, 15, 744–751.
- [71] W. P. Thurston, *Geometry Topol. Monogr.* **1998**, 1, 511–549, The Epstein Birthday Schrift.

- [72] P. Schwerdtfeger, L. Wirz, J. Avery, *J. Comput. Chem.* **2013**, *34*, 1508–1526.
- [73] L. N. Wirz, R. Tonner, J. Avery, P. Schwerdtfeger, *J. Chem. Inf. Model.* **2014**, *54*, 121–130.
- [74] G. Brinkmann, J. Goedgebeur, H. Mélot, K. Coolsaet, *Discrete Appl. Math.* **2013**, *161*, 311–314.
- [75] H. W. Kroto, *Nature* **1987**, *329*, 529–531.
- [76] M. Dutour, M. Deza, *Electron. J. Comb.* **2004**, *11*, 1–49.
- [77] A. L. Mackay, *Acta Crystallogr.* **1962**, *15*, 916–918.
- [78] H.-S. Nam, N. M. Hwang, B. D. Yu, J.-K. Yoon, *Phys. Rev. Lett.* **2002**, *89*, 275502.
- [79] L. N. Wirz, R. Tonner, A. Hermann, R. Sure, P. Schwerdtfeger, *J. Comput. Chem.* **2016**, *37*, 10–17.
- [80] J. P. Perdew, *Phys. Rev. B* **1986**, *33*, 8822.
- [81] A. D. Becke, *Phys. Rev. A* **1988**, *38*, 3098–3100.
- [82] S. Grimme, J. Antony, S. Ehrlich, H. Krieg, *J. Chem. Phys.* **2010**, *132*, 154104.
- [83] S. Grimme, S. Ehrlich, L. Goerigk, *J. Comput. Chem.* **2011**, *32*, 1456–1465.
- [84] P. J. Hay, W. R. Wadt, *J. Chem. Phys.* **1985**, *82*, 299–310.
- [85] L. A. Mancera, D. M. Benoit, *Comput. Theor. Chem.* **2015**, *1067*, 24–32.
- [86] D. Figgen, G. Rauhut, M. Dolg, H. Stoll, *Chem. Phys.* **2005**, *311*, 227–244, Relativistic Effects in Heavy-Element Chemistry and Physics, in *Memoriam Bernd A. Hess (1954–2004)*.
- [87] K. A. Peterson, C. Puzzarini, *Theor. Chem. Acc.* **2005**, *114*, 283–296.
- [88] D. Schooss, P. Weis, O. Hampe, M. M. Kappes, *Philos. Trans. R. Soc. London Ser. A* **2010**, *368*, 1211–1243.
- [89] A. Lechtken, C. Neiss, M. M. Kappes, D. Schooss, *Phys. Chem. Chem. Phys.* **2009**, *11*, 4344–4350.
- [90] F. Weigend, R. Ahlrichs, *Phys. Chem. Chem. Phys.* **2005**, *7*, 3297–3305.
- [91] TURBOMOLE V7.0 2015, a development of University of Karlsruhe and Forschungszentrum Karlsruhe GmbH, 1989–2007, TURBOMOLE GmbH, since 2007; available from <http://www.turbomole.com>.
- [92] G. Kresse, J. Furthmüller, *Comp. Math. Sci.* **1996**, *6*, 15.
- [93] P. E. Blöchl, *Phys. Rev. B* **1994**, *50*, 17953.
- [94] G. Kresse, D. Joubert, *Phys. Rev. B* **1999**, *59*, 1758.
- [95] A. F. Jalbout, F. F. Contreras-Torres, L. A. Pérez, I. L. Garzón, *J. Phys. Chem. A* **2008**, *112*, 353–357.
- [96] M. Laupp, J. Strähle, *Angew. Chem. Int. Ed. Engl.* **1994**, *33*, 207–209; *Angew. Chem.* **1994**, *106*, 210–211.
- [97] N. Takeuchi, C. T. Chan, K. M. Ho, *Phys. Rev. B* **1989**, *40*, 1565–1570.
- [98] The larger golden fullerene Au₃₂, Au₅₀, and Au₇₂ have been studied theoretically by Johansson et al., see: M. P. Johansson, J. Vaara, D. Sundholm, *J. Phys. Chem. C* **2008**, *112*, 19311–19315.

Received: March 15, 2016

Published online on May 31, 2016

Please note: Minor changes have been made to this manuscript since its publication in *Chemistry—A European Journal* Early View. The Editor.